SC-FDMA versus OFDMA: Sensitivity to Large Carrier Frequency and Timing Offsets on the Uplink

K. Raghunath and A. Chockalingam
Department of ECE, Indian Institute of Science, Bangalore 560012, INDIA

Abstract— **In this paper, we present a comparison between the sensitivity of SC-FDMA and OFDMA schemes to large carrier frequency offsets (CFO) and timing offsets (TO) of different users on the uplink. Our study shows the following observations: 1) In the ideal case of zero CFOs and TOs (i.e., perfect synchronization), the uncoded BER performance of SC-FDMA with frequency domain MMSE equalizer is better than that of OFDMA due to the inherent frequency diversity that is possible in SC-FDMA. Also, because of inter-symbol interference in SC-FDMA, the performance of SC-FDMA with MMSE equalizer can be further improved by using low-complexity interference cancellation (IC) techniques. 2) In the presence of large CFOs and TOs, significant multiuser interference (MUI) gets introduced, and hence the performance of SC-FDMA with MMSE equalizer can get worse than that of OFDMA. However, the performance advantage of SC-FDMA with MMSE equalizer over OFDMA (due to the potential for frequency diversity benefit in SC-FDMA) can be restored by adopting multistage IC techniques, using the knowledge of CFOs and TOs of different users at the receiver.**

Keywords – *SC-FDMA, OFDMA, carrier frequency offset, timing offset, multiuser interference, interference cancellation.*

I. Introduction

In order to alleviate the peak-to-average power ratio (PAPR) problem encountered in uplink OFDMA (orthogonal frequency division multiple access [1]), SC-FDMA (single carrier frequency division multiple access [2]-[4]) has been adopted for uplink transmission in UTRA LTE [5]-[7]. Another drawback in OFDMA is its inherent loss of frequency diversity, which can be alleviated by using some form of precoding. SC-FDMA can be viewed as a precoded OFDMA scheme, where the precoding is done by means of a DFT matrix. This M-point DFT precoding operation at the transmitter results in all M data symbols of a user to be mounted on all its M subcarriers, and with independent fades on these subcarriers, achieving frequency diversity becomes possible. With appropriate frequency domain equalization at the receiver (e.g., MMSE equalizer), SC-FDMA can achieve performance gains due to frequency diversity. In addition to providing low PAPR compared to OFDMA and frequency diversity, SC-FDMA allows flexible sharing of spectrum between different users.

With the adoption of SC-FDMA in UTRA LTE, studies concerning different aspects of SC-FDMA are increasingly being reported in the recent literature [8]-[12]. A simulated coded block error rate performance comparison between SC-FDMA with frequency domain MMSE equalization and OFDMA, evaluated for various modulation and coding sets specified in UTRA LTE, is presented in [8]; OFDMA is shown to perform better than SC-FDMA for some modulation and coding sets. Subsequently, the same authors, in [9], proposed a iterative equalization and decoding (turbo equalization) scheme, and showed that SC-FDMA with turbo equalizer performed better than (or same as) OFDMA for all modulation and coding sets considered. On a similar line, the authors in [10] proposed a soft-output trellis based equalizer that takes into account the cyclic inter-symbol interference (ISI) structure arising in SC-FDMA, and showed that SC-FDMA with trellis based equalizer performed better than SC-FDMA with MMSE equalization. An approximate performance analysis of the BER of SC-FDMA with frequency domain equalization is presented in [11]. In [12], a PAPR and BER performance comparison between SC-FDMA, OFDMA and Walsh-Hadamard precoded OFDMA is presented, where the PAPR advantage of SC-FDMA in the presence of power amplifier non-linearity has been analyzed.

In the above papers on SC-FDMA, perfect frequency and timing alignment has been assumed. However, as in uplink OFDMA [13], carrier frequency offsets (CFO) and timing offsets (TO) are encountered in SC-FDMA as well; CFOs are induced by Doppler effects and/or poor oscillator alignments, and TOs are caused due to path delay differences between different users and imperfect timing synchronization. Large CFOs and TOs can cause significant multiuser interference (MUI) in uplink OFDMA[1] and SC-FDMA. Sensitivity of OFDMA performance to CFOs and TOs has been reported in the literature [16]; also, interference canceling receivers to alleviate the detrimental effects of large CFOs/TOs in uplink OFDMA have been proposed [13]-[16]. However, to our knowledge, such a CFO/TO sensitivity study has not been reported so far for SC-FDMA. It is of interest to compare the performance of SC-FDMA with that of OFDMA in the presence of large CFOs and TOs, which forms the main focus of this paper. Our contributions in this paper can be summarized as follows: 1) we derive analytical expressions for the various CFO/TO induced interferences in SC-FDMA, 2) using these expressions, we devise a multistage parallel interference canceller (PIC) that enables to recover the frequency diversity effect that is lost due to the CFO/TO induced interferences, and 3) our simulation results show that, in the presence of large CFOs and TOs, because of significant MUI introduced due to CFOs/TOs, the performance of SC-FDMA with MMSE equalizer can get worse than that of OFDMA; however, the performance advantage of SC-FDMA over OFDMA (due to the potential for frequency diversity benefit in SC-FDMA) can be restored by the proposed PIC receiver.

[1] In practice, the detrimental effects of CFOs and TOs in uplink OFDMA are avoided through tight closed-loop frequency/timing correction between the mobile transmitters and the base station (BS) receiver [17]. An alternate approach to handle CFO/TO effects is to use interference cancellation at BS receiver, which can save on feedback bandwidth and oscillator cost [13]-[15].

This work was supported in part by the DRDO-IISc Program on Advanced Research in Mathematical Engineering.

978-1-4244-4148-8/09/$25.00 ©2009

II. System Model

We consider a system with K users and N subcarriers. M subcarriers, $M = N/K$, are allocated to each user where each subcarrier is allocated to only one user, either in contiguous blocks (block allocation), or in an interleaved fashion (interleaved allocation). We consider L-path frequency selective and quasi-static independent channels between users and the BS, with each path coefficient to be an i.i.d complex Gaussian random variable with variance $\frac{1}{L}$. Let[2]

$$\mathbf{x}^u = [x_0^u \; x_1^u \; x_2^u \; \cdots \; x_{M-1}^u]^T, \quad (1)$$

denote the uth user's complex data symbol frame of size M, with each symbol x_i^u drawn from a QAM constellation. Denoting the M-point DFT matrix by $\mathbf{D}^M$, the set of subcarriers allocated to the uth user by $\mathcal{S}_u$, the subcarrier allocation matrix of order $N \times M$ by $\mathbf{A}^u$ where

$$\mathbf{A}^u_{q,k} = \begin{cases} 1, & \text{if } q \in \mathcal{S}_u \text{ and input to } q\text{th subcarrier} \\ & \text{is the } k\text{th element of } \mathbf{D}^M\mathbf{x}^u, \\ 0, & \text{if } q \notin \mathcal{S}_u, \end{cases} \quad (2)$$

and the N-point IDFT matrix by $\widetilde{\mathbf{D}}^N$, the output of the N-point IDFT unit of the uth user (in Fig. 1) can be as

$$\mathbf{s}^u = \widetilde{\mathbf{D}}^N\mathbf{A}^u\mathbf{D}^M\mathbf{x}^u. \quad (3)$$

The IDFT output vector $\mathbf{s}^u$ is transmitted after adding the cyclic prefix. The length of the cyclic prefix, N_g, is equal to the delay spread of the channel, $L-1$. The transmitted frame gets linearly convolved with the channel impulse response (CIR) of the uth user, $\mathbf{h}^u$, and reaches the BS receiver.

A. Receiver with perfect carrier frequency/timing alignment

Assuming perfect timing and carrier frequency alignment (i.e., no CFO and TO) at the receiver, the input to the N-point DFT at the receiver, after dropping the cyclic prefix, is given by

$$\mathbf{y} = \sum_{u=1}^{K} \mathbf{s}^u \star \mathbf{h}^u + \mathbf{z}^u, \quad (4)$$

where $\star$ indicates N-point circular convolution. The output of the N-point DFT due to the signal from all the users can be expressed as

$$\mathbf{y}_F = \sum_{u=1}^{K} \mathbf{H}^u\mathbf{A}^u\mathbf{D}^M\mathbf{x}^u + \mathbf{z}_F, \quad (5)$$

where $\mathbf{H}^u$ is a diagonal matrix of order $N \times N$ with

$$\mathbf{H}^u_{k,k} = \sum_{n=0}^{L-1} h_n^u e^{\frac{-j2\pi(k-1)n}{N}}, \quad (6)$$

and $\mathbf{z}_F$ is the output noise vector due to the input noise vector, $\sum_{u=1}^{K}\mathbf{z}^u$. Denoting the variances of the signal and noise by σ_s^2 and σ_n^2, respectively, at the output of N-point DFT, the frequency domain MMSE equalizer [3] of uth user is a diagonal matrix $\widetilde{\mathbf{H}}^u$ of order $N \times N$ with

$$\widetilde{\mathbf{H}}^u_{k,k} = \frac{(\mathbf{H}^u_{k,k})^*}{|\mathbf{H}^u_{k,k}|^2 + \frac{\sigma_n^2}{\sigma_s^2}}. \quad (7)$$

Defining $\widetilde{\mathbf{A}}^u = [\mathbf{A}^u]^T$ as the deallocation matrix of uth user, the input to the M-point IDFT of the vth user is

$$\mathbf{r}^v = \widetilde{\mathbf{A}}^v\widetilde{\mathbf{H}}^v\Big(\mathbf{H}^v\mathbf{A}^v\mathbf{D}^M\mathbf{x}^v + \sum_{\substack{u=1 \\ u\neq v}}^{K} \mathbf{H}^u\mathbf{A}^u\mathbf{D}^M\mathbf{x}^u + \mathbf{z}_F\Big). \quad (8)$$

Since

$$\widetilde{\mathbf{A}}^v\mathbf{A}^u = \begin{cases} \mathbf{I}_{M\times M}, & \text{if } v = u \\ \phi, & \text{otherwise,} \end{cases} \quad (9)$$

for $v \neq u$, $\widetilde{\mathbf{A}}^v\widetilde{\mathbf{H}}^u\mathbf{H}^u\mathbf{A}^u$ is a null matrix, and so

$$\mathbf{r}^v = \widetilde{\mathbf{A}}^v\widetilde{\mathbf{H}}^v\Big(\mathbf{H}^v\mathbf{A}^v\mathbf{D}^M\mathbf{x}^v + \mathbf{z}_F\Big). \quad (10)$$

Denoting the M-point IDFT matrix by $\widetilde{\mathbf{D}}^M$, the output of M-point IDFT of the vth user is

$$\widetilde{\mathbf{x}}^v = \underbrace{\widetilde{\mathbf{D}}^M\widetilde{\mathbf{A}}^v\widetilde{\mathbf{H}}^v\mathbf{H}^v\mathbf{A}^v\mathbf{D}_M}_{\triangleq \mathbf{F}^v}\mathbf{x}^v + \widetilde{\mathbf{D}}^M\widetilde{\mathbf{A}}^v\widetilde{\mathbf{H}}^v\mathbf{z}_F. \quad (11)$$

In (11), $\mathbf{F}^v$ is a square matrix of order $M \times M$ with

$$\mathbf{F}^v_{n,r} = \frac{1}{M}\sum_{k=0}^{M-1} \frac{|\mathbf{H}^v_{k'}|^2}{|\mathbf{H}^v_{k'}|^2 + \frac{\sigma_n^2}{\sigma_s^2}} e^{\frac{j2\pi k(n-r)}{M}}, \quad (12)$$

where k' for the vth user is given by

$$k' = \begin{cases} M(v-1)+k, & \text{for block allocation,} \\ Kk+v-1, & \text{for interleaved allocation.} \end{cases} \quad (13)$$

Due to the MMSE equalization in (7), we can see in (11) that each symbol at the output is affected by the interference from the other symbols of the same user, which we refer to as MMSE-SI (MMSE self interference). Defining the diagonal matrix $\mathbf{\Lambda}^v$ of order $M \times M$ as

$$\mathbf{\Lambda}^v = diag[\mathbf{F}^v], \quad (14)$$

the desired signal, MMSE-SI and noise terms in (11) can be shown separately as

$$\widetilde{\mathbf{x}}^v = \underbrace{\mathbf{\Lambda}^v\mathbf{x}^v}_{\text{Desired signal}} + \underbrace{(\mathbf{F}^v - \mathbf{\Lambda}^v)\mathbf{x}^v}_{\text{MMSE-SI}} + \underbrace{\widetilde{\mathbf{A}}^v\widetilde{\mathbf{H}}^v\mathbf{z}_F}_{\text{Noise}}. \quad (15)$$

Therefore, the M-point IDFT output expression for the nth symbol of the vth user is of the form

$$\widetilde{\mathbf{x}}^v_n = \underbrace{\mathbf{x}^v_n\mathbf{F}^v_{n,n}}_{\text{Desired signal}} + \underbrace{\sum_{\substack{r=0 \\ r\neq n}}^{M-1} \mathbf{x}^v_r\mathbf{F}^v_{n,r}}_{\text{MMSE-SI}} + \underbrace{\frac{1}{M}\sum_{k=0}^{M-1} \frac{(\mathbf{H}^v_{k'})^*}{|\mathbf{H}^v_{k'}|^2 + N_o} z_{F_{k'}} e^{\frac{j2\pi kn}{M}}}_{\text{Noise}}. \quad (16)$$

[2]We use boldface small letters to represent vectors, and boldface capital letters to represent matrices. We refer to a general user as uth user and the desired user as vth user. $(.)^*$ and $(.)^T$ denote the conjugate and transpose operation, respectively

978-1-4244-4148-8/09/$25.00 ©2009
This full text paper was peer reviewed at the direction of IEEE Communications Society subject matter experts for publication in the IEEE "GLOBECOM" 2009 proceedings.

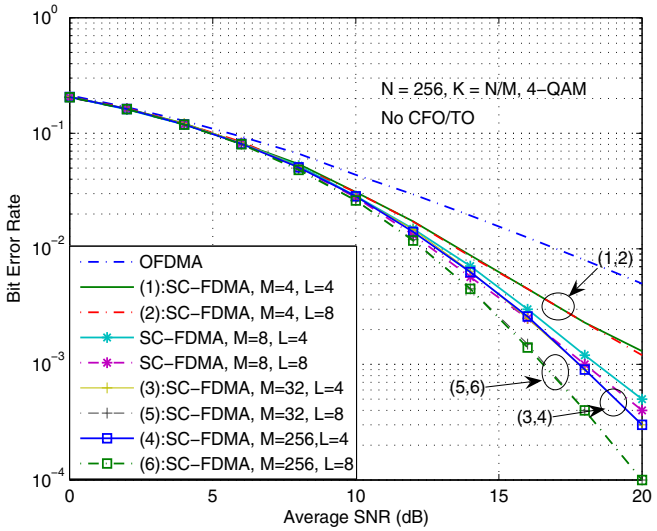

Fig. 1. Comparison of uncoded BER performance of SC-FDMA and OFDMA with no CFO and TO. $N = 256$, $M = 4, 8, 32, 256$, $K = N/M$, $L = 4, 8$, 4-QAM, and interleaved allocation, *SC-FDMA outperforms OFDMA due its frequency diversity advantage*.

In (16), we can see that uplink SC-FDMA with MMSE equalizer is providing frequency diversity and its BER performance can be improved by doing one or more of the following: 1) Increasing M which increases the number of subcarriers on which each symbol is sent. This reduces the frequency separation between adjacent subcarriers. When the separation becomes less than the coherence bandwidth, the correlation between the frequency response coefficients and the number of subcarriers causing MMSE-SI will increase causing the saturation in the improvement of BER performance. 2) Increasing the separation between the subcarriers, which can be done by interleaved allocation. Apart from this, if L gets increased, it makes the channel more frequency selective, thus reducing the correlation in $H_{k'}$'s. But if the subcarriers are already independent, increase in L will not improve the BER.

Note that the frequency domain equalized N-point DFT output for the uplink OFDMA system can be obtained from (11) as a special case, by making $\mathbf{D}^M = \widetilde{\mathbf{D}}^M = \mathbf{I}_{M\times M}$ and $\widetilde{\mathbf{H}}^v_{k,k} = \frac{(\mathbf{H}^v_{k,k})^*}{|\mathbf{H}^v_{k,k}|^2}$. With this substitution, $\mathbf{F}^v$ in (11) becomes $\mathbf{I}_{M\times M}$ and the output vector becomes

$$\widetilde{\mathbf{x}}^v \;=\; \mathbf{x}^v + \widetilde{\mathbf{A}}^v\widetilde{\mathbf{H}}^v\mathbf{z}_F. \tag{17}$$

In (17), we can see that OFDMA does not provide any form of diversity and is not affected by interference when the system is perfectly synchronized.

B. SC-FDMA vs OFDMA performance under No CFO/TO

In Fig. 1, we plot the simulated uncoded BER performance of SC-FDMA and OFDMA with the parameters given in the figure. Figure 1 shows that the BER performance of OFDMA remains the same for all M and L (because of no frequency diversity in OFDMA), but in the case of SC-FDMA, for a given M, the BER improves with increasing L (if the increase in L can reduce the correlation between the frequency response coefficients). This uncoded BER performance advantage of SC-FDMA over OFDMA is due to the inherent frequency diversity in SC-FDMA.

III. SC-FDMA with Non-zero CFOs and TOs

In this section, we consider uplink SC-FDMA with imperfect carrier/timing alignment (i.e., with non-zero CFOs and TOs).

A. Case of Non-zero CFOs and No TOs

First, consider the case with non-zero CFO and no TO (i.e., perfect timing). The uth user's CFO, normalized by the subcarrier spacing, is denoted by ϵ_u, $0 \le \epsilon_u \le 0.5$. To characterize the effect of CFO on the signal received from uth user, we define the diagonal matrix $\mathbf{V}^u$ of order $N \times N$ with

$$\mathbf{V}^u_{n,n} \;=\; e^{\frac{j2\pi\epsilon_u(n-1)}{N}}. \tag{18}$$

The input to the N-point DFT at the receiver, after dropping the cyclic prefix, is

$$\mathbf{y} \;=\; \sum_{u=1}^{K}\mathbf{V}^u(\mathbf{s}^u \star \mathbf{h}^u) + \mathbf{z}^u. \tag{19}$$

The output of N-point DFT is

$$\mathbf{y}_F \;=\; \sum_{u=1}^{K}\Psi^u\mathbf{H}^u\mathbf{A}^u\mathbf{D}^M\mathbf{x}^u + \mathbf{z}_F, \tag{20}$$

where Ψ^u is a circulant matrix with

$$\Psi^u_{k,q} = \frac{1}{N}\sum_{n=0}^{N-1} e^{\frac{j2\pi(\epsilon_u+q-k)n}{N}}. \tag{21}$$

After MMSE equalization and deallocation, the input to the M-point IDFT of the vth user is

$$\mathbf{r}^v = \widetilde{\mathbf{A}}^v\widetilde{\mathcal{H}}^v\Big(\underbrace{\Psi^v_{1,1}\mathbf{H}^v}_{\triangleq\,\mathcal{H}^v}\mathbf{A}^v\mathbf{D}^M\mathbf{x}^v + \left(\Psi^v - \Psi^v_{1,1}\mathbf{I}_{N\times N}\right)\mathbf{H}^v\mathbf{A}^v\mathbf{D}^M\mathbf{x}^u + \sum_{\substack{u=1\\u\neq v}}^{K}\Psi^u\mathbf{H}^u\mathbf{A}^u\mathbf{D}^M\mathbf{x}^u + \mathbf{z}_F\Big), \tag{22}$$

where $\widetilde{\mathcal{H}}^v$ is a $N \times N$ diagonal matrix with

$$\widetilde{\mathcal{H}}^v_{k,k} \;=\; \frac{(\mathcal{H}^v_{k,k})^*}{|\mathcal{H}^v_{k,k}|^2 + \frac{\sigma_n^2}{\sigma_s^2}}. \tag{23}$$

The M-point IDFT output of the vth user is

$$\begin{aligned}\widetilde{\mathbf{x}}^v \;=\;& \widetilde{\mathbf{D}}^M\widetilde{\mathbf{A}}^v\widetilde{\mathcal{H}}^v\mathcal{H}^v\mathbf{A}^v\mathbf{D}^M\mathbf{x}^v \\ &+ \widetilde{\mathbf{D}}^M\widetilde{\mathbf{A}}^v\widetilde{\mathcal{H}}^v\left(\Psi^v - \Psi^v_{1,1}\mathbf{I}_{N\times N}\right)\mathbf{H}^v\mathbf{A}^v\mathbf{D}^M\mathbf{x}^v \\ &+ \widetilde{\mathbf{D}}^M\widetilde{\mathbf{A}}^v\widetilde{\mathcal{H}}^v\sum_{\substack{u=1\\u\neq v}}^{K}\Psi^u\mathbf{H}^u\mathbf{A}^u\mathbf{D}^M\mathbf{x}^u + \widetilde{\mathbf{D}}^M\widetilde{\mathbf{A}}^v\widetilde{\mathcal{H}}^v\mathbf{z}_F.\end{aligned} \tag{24}$$

If the vth user's CFO is compensated at the front-end of the receiver, Ψ^v becomes $\mathbf{I}_{N\times N}$, and the output becomes

$$\begin{aligned}\widetilde{\mathbf{x}}^v \;=\;& \underbrace{\mathbf{\Lambda}^v\mathbf{x}^v}_{\text{Desired signal}} + \underbrace{(\mathbf{F}^v - \mathbf{\Lambda}^v)\mathbf{x}^v}_{\text{MMSE-SI}} \\ &+ \underbrace{\widetilde{\mathbf{D}}^M\widetilde{\mathbf{A}}^v\mathbf{H}^v\sum_{\substack{u=1\\u\neq v}}^{K}\tilde{\Psi}^u\mathbf{H}^u\mathbf{A}^u\mathbf{D}^M\mathbf{x}^u}_{\text{MUI}} + \underbrace{\widetilde{\mathbf{D}}^M\widetilde{\mathbf{A}}^v\mathbf{H}^v\mathbf{z}_F}_{\text{Noise}},\end{aligned} \tag{25}$$

978-1-4244-4148-8/09/$25.00 ©2009
This full text paper was peer reviewed at the direction of IEEE Communications Society subject matter experts for publication in the IEEE "GLOBECOM" 2009 proceedings.

where $\widetilde{\Psi}^u$ is nothing but Ψ^u in which ϵ_u is replaced with $\epsilon_u - \epsilon_v$. In (25), we can see that with perfect timing and non-zero CFOs, apart from MMSE-SI, due to the loss of orthogonality among the subcarriers of the desired user and the other users, each output symbol is affected by MUI from all the other users. The output expression for OFDMA can be obtained as a special case of (25) with the substitution used to obtain (17).

B. Case of Non-zero CFOs and TOs

Now, consider the case with non-zero CFOs as well as TOs. The uth user's TO is denoted by μ_u, in number of samples. In order to account for TOs in the output expressions, depending on the values of μ_u's, we need to consider four different cases of timing offsets $\big($cases *a)* to *d)* to be described later$\big)$, where interference is caused by CFO in all the paths, and the previous or next frame interference along with current frame interference in some or all the paths depending on the magnitude and sign of the TO. Apart from this, self interference is also caused due to MMSE equalization. With vth user as the desired user, any interference due to the signal from vth user is referred to as the self interference (SI), and due to the signal from other user is referred to as the MUI. We refer to the interference caused due to: $i)$ only CFO by *'CFO-SI/MUI'*, $ii)$ both CFO and the loss of some samples in the current frame by *'CF-SI/MUI'*, $iii)$ CFO and symbols in the previous frame by *'PF-SI/MUI'*, $iv)$ CFO and symbols in the next frame by *'NF-SI/MUI'*, and $v)$ MMSE equalization by *'MMSE-SI/MUI'. It is noted that the MMSE equalization induced interferences (i.e., MMSE-SI/MUI) will not be there in OFDMA [16], and these extra interference terms in SC-FDMA, if not cancelled using suitable IC techniques, will cause increased performance degradation in SC-FDMA compared to OFDMA in the presence of non-zero CFOs/TOs (as will be shown in the SINR/BER performance plots in Sec. V).*

The N-point DFT output of the uth user at the receiver, due to uth user's signal in the presence of non-zero CFO/TO is given by

$$\mathbf{y}_F^u = \underbrace{\mathbf{G}^u\mathbf{A}^u\mathbf{D}^M\mathbf{x}^u}_{\mathbf{y}^{u,DS}+\mathbf{y}^{u,CI}} + \underbrace{\mathbf{G}^{u,I}\mathbf{A}^u\mathbf{D}^M\mathbf{x}^{u,I}}_{\mathbf{y}^{u,I}} + \underbrace{\mathbf{z}_F^u}_{\text{Noise}}, \quad (26)$$

where $\mathbf{y}^{u,DS}$ is the desired signal, $\mathbf{y}^{u,CI}$ is the current frame interference, and $\mathbf{y}^{u,I}$ is previous or next frame interference. $\mathbf{x}^u$ is the current frame and $\mathbf{x}^{u,I}$ is the interfering frame of the uth user, which is the next frame if the timing offset is positive and previous frame if the the timing offset is negative. $\mathbf{G}^u$ and $\mathbf{G}^{u,I}$ are the frequency response matrices for the current and interfering frames, respectively, for the uth user, determined by the channel impulse responses and the values of timing and carrier frequency offsets of uth user. In all the cases of timing offset we assume constant CIR in the processing window, use l as the path index and define

$$\Gamma_{qk}^{u,l}(n_1,n_2) \triangleq \frac{1}{N}\sum_{n=n_1}^{n_2} e^{\frac{j2\pi n(q-k+\epsilon_u)}{N}}, \quad (27)$$

and

$$\mathbf{G}_{k,q}^u = e^{\frac{i2\pi\mu_u q}{N}}\sum_{l=0}^{L-1} h_l^u e^{\frac{-i2\pi lq}{N}}\Gamma_{qk}^{u,l}(n_1,n_2). \quad (28)$$

The different cases of TOs to be considered are as follows:

- *Case a)*: $0 < -\mu_u \leq N_g$, where CFO-SI/MUI is caused for $l \leq N_g + \mu_u$. $l - N_g - \mu$ samples of the previous frame come into the processing window for $l > N_g + \mu_u$ causing PF-SI/MUI. Also because of the loss of $l - N_g - \mu$ samples in the current frame, CF-SI/MUI is caused. The channel matrix for the previous frame is

$$\mathbf{G}_{k,q}^{u,I} = e^{\frac{i2\pi(\mu_u+N_g)q}{N}}\sum_{l=N_g+\mu_u+1}^{L-1} h_l^u e^{\frac{-i2\pi lq}{N}}\Gamma_{qk}^{u,l}(0,n_1-1), \quad (29)$$

with

$$(n_1,n_2) = \begin{cases} (0,N-1), & \text{for } l \leq N_g+\mu_u, \\ (l-\mu_u-N_g,N-1), & \text{for } l > N_g+\mu_u. \end{cases} \quad (30)$$

Here, $\mathbf{y}^{u,CI}$ is the sum of CFO-SI/MUI and CF-SI/MUI, and $\mathbf{y}^{u,I}$ is PF-SI/MUI.

- *Case b)*: $N_g < -\mu$, where CF-SI/MUI and PF-SI/MUI occurs for all the paths. The channel matrix for the previous frame is same as (29), with the limits in the summation being $(0, L-1)$ in $\mathbf{G}_{k,q}^{u,I}$, with

$$(n_1,n_2) = (l-\mu_u-N_g, N-1). \quad (31)$$

Here, $\mathbf{y}^{u,CI}$ is CF-SI/MUI, and $\mathbf{y}^{u,I}$ is PF-SI/MUI.

- *Case c)*: $0 < \mu < L$, where $\mu_u - l$ samples of the next frame come into the processing window for paths $l \leq \mu_u - 1$, causing NF-SI/MUI, and the same number of samples of the current frame are lost causing CF-SI/MUI. For $l > \mu_u - 1$, CFO-SI/MUI is caused. The channel matrix for the next frame is

$$\mathbf{G}_{k,q}^{u,I} = e^{\frac{-i2\pi(N_g-\mu_u)q}{N}}\sum_{l=0}^{\mu_u-1} h_l^u e^{\frac{-i2\pi lq}{N}}\Gamma_{qk}^{u,l}(n_2+1,N-1), \quad (32)$$

with

$$(n_1,n_2) = \begin{cases} (0,N-1-\mu_u+l), & \text{for } 0 \leq l \leq \mu_u-1, \\ (0,N-1), & \text{for } l \geq \mu_u. \end{cases} \quad (33)$$

Here, $\mathbf{y}^{u,CI}$ is the sum of CFO-SI/MUI and CF-SI/MUI, and $\mathbf{y}^{u,I}$ is NF-SI/MUI.

- *Case d)*: $\mu \geq L$, where NF-SI/MUI and CF-SI/MUI occur for all the paths. In this case the channel matrix for the next frame is same as (32), with the limits in the summation being $(0, L-1)$ in $\mathbf{G}_{k,q}^{u,I}$, with

$$(n_1,n_2) = (0, N-1+l-\mu_u). \quad (34)$$

Here $\mathbf{y}^{u,CI}$ is CF-SI/MUI, and $\mathbf{y}^{u,I}$ is PF-SI/MUI.

Since DFT is a linear operation, total N-point DFT output at the receiver is given by

$$\mathbf{y}_F = \sum_{u=1}^{K}\mathbf{y}_F^u. \quad (35)$$

978-1-4244-4148-8/09/$25.00 ©2009
This full text paper was peer reviewed at the direction of IEEE Communications Society subject matter experts for publication in the IEEE "GLOBECOM" 2009 proceedings.

The input to the M-point IDFT of the vth user is

$$\mathbf{r}^v = \widetilde{\mathbf{A}}^v\widetilde{\mathbf{G}}^{v,d}\Big(\mathbf{G}^{v,d}\mathbf{A}^v\mathbf{D}^M\mathbf{x}^v + (\mathbf{G}^v - \mathbf{G}^{v,d})\mathbf{A}^v\mathbf{D}^M\mathbf{x}^v + \mathbf{G}^{v,I}\mathbf{A}^v\mathbf{D}^M\mathbf{x}^{v,I} + \sum_{\substack{u=1\\u\neq v}}^{K}\mathbf{y}_F^u + \mathbf{z}_F\Big), \quad (36)$$

where $\mathbf{G}^{v,d}$ and $\widetilde{\mathbf{G}}^{v,d}$ are $N \times N$ the diagonal matrices with

$$\mathbf{G}^{v,d} = diag[\mathbf{G}^v], \quad (37)$$

and

$$\widetilde{\mathbf{G}}_{k,k}^{v,d} = \frac{(\mathbf{G}_{k,k}^{v,d})^*}{|\mathbf{G}^{v,d}(k,k)|^2 + \frac{\sigma_n^2}{\sigma_s^2}}. \quad (38)$$

The M-point IDFT output of the vth user can be written as

$$\widetilde{\mathbf{x}}^v = \underbrace{\widetilde{\mathbf{D}}^M\widetilde{\mathbf{A}}^v\widetilde{\mathbf{G}}^{v,d}\mathbf{G}^{v,d}\mathbf{A}^v\mathbf{D}^M}_{\triangleq\,\mathcal{F}^v}\mathbf{x}^v + \widetilde{\mathbf{D}}^M\widetilde{\mathbf{A}}^v\widetilde{\mathbf{G}}^{v,d}(\mathbf{G}^v - \mathbf{G}^{v,d})\mathbf{A}^v\mathbf{D}^M\mathbf{x}^v + \widetilde{\mathbf{D}}^M\widetilde{\mathbf{A}}^v\widetilde{\mathbf{G}}^{v,d}\mathbf{G}^{u,I}\mathbf{A}^v\mathbf{D}^M\mathbf{x}^{v,I} + \widetilde{\mathbf{D}}^M\widetilde{\mathbf{A}}^v\widetilde{\mathbf{G}}^{v,d}\Big(\sum_{\substack{u=1\\u\neq v}}^{K}\mathbf{y}_F^u + \mathbf{z}_F\Big)\Big). \quad (39)$$

Defining a diagonal matrix $\mathcal{D}^v$ as

$$\mathcal{D}^v = diag[\mathcal{F}^v], \quad (40)$$

we can write (39) in terms of various interference terms as

$$\widetilde{\mathbf{x}}^v = \underbrace{\mathcal{D}^v\mathbf{x}^v}_{\text{Desired signal}} + \underbrace{(\mathcal{F}^v - \mathcal{D}^v)\mathbf{x}^v}_{\text{MMSE-SI}} + \underbrace{\widetilde{\mathbf{D}}^M\widetilde{\mathbf{A}}^v\widetilde{\mathbf{G}}^{v,d}(\mathbf{G}^v - \mathbf{G}^{v,d})\mathbf{A}^v\mathbf{D}_M\mathbf{x}^v}_{\text{CF-SI}} + \underbrace{\widetilde{\mathbf{D}}^M\widetilde{\mathbf{A}}^v\widetilde{\mathbf{G}}^{v,d}\mathbf{G}^{v,I}\mathbf{A}^v\mathbf{D}_M\mathbf{x}^{v,I}}_{\text{PF-SI/NF-SI}} + \underbrace{\widetilde{\mathbf{D}}^M\widetilde{\mathbf{A}}^v\widetilde{\mathbf{G}}^{v,d}\Big(\sum_{\substack{u=1\\u\neq v}}^{K}\mathbf{y}_F^u + \mathbf{z}_F\Big)}_{\text{MUI + Noise}}. \quad (41)$$

The corresponding output expression for OFDMA can be obtained as a special case of (41) with the substitution used to obtain (17).

C. Proposed Parallel Interference canceler

We propose to use a parallel interference canceler (PIC) at the BS receiver to mitigate the effect of interferences in SC-FDMA. Using estimates of the interfering symbols and the channel fade coefficients, we can reconstruct the ISI and MUI terms which then can be subtracted from the received signal to achieve interference cancellation. For illustration, consider the case of non-zero CFOs. In the first stage of the receiver, no cancellation is done and the symbols of all the users are detected at the M-point DFT output. In the mth PIC stage, $m \geq 2$, the symbols are detected using

$$\widetilde{\mathbf{x}}^{v,m} = \mathbf{\Lambda}^v\mathbf{x}^v + (\mathbf{F}^v - \mathbf{\Lambda}^v)(\mathbf{x}^v - \widehat{\mathbf{x}}^{v,m-1}) + \widetilde{\mathbf{D}}^M\widetilde{\mathbf{A}}^v\mathbf{H}^v\sum_{\substack{u=1\\u\neq v}}^{K}\Psi^{(u)}\mathbf{H}^u\mathbf{A}^u\mathbf{D}^M(\mathbf{x}^u - \widehat{\mathbf{x}}^{u,m-1}) + \widetilde{\mathbf{D}}^M\widetilde{\mathbf{A}}^v\mathbf{H}^v\mathbf{z}_F, \quad (42)$$

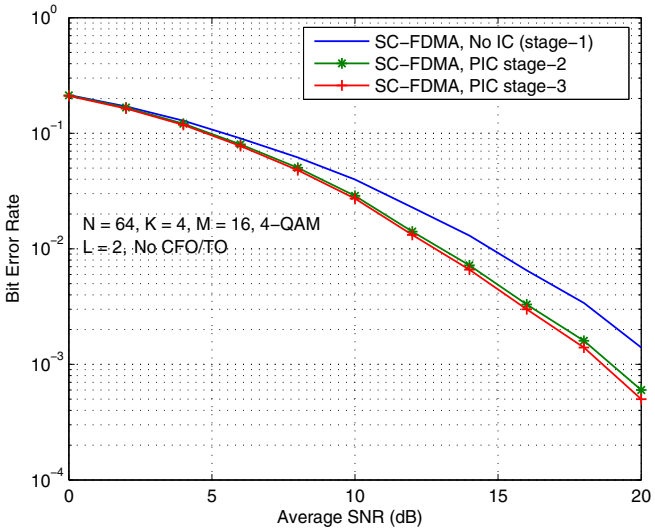

Fig. 2. BER performance of SC-FDMA without and with IC cancellation. $N = 64$, $K = 4$, $M = 16$, $L = 2$, 4-QAM, No CFO and TO. *IC removes residual interference and improves performance.*

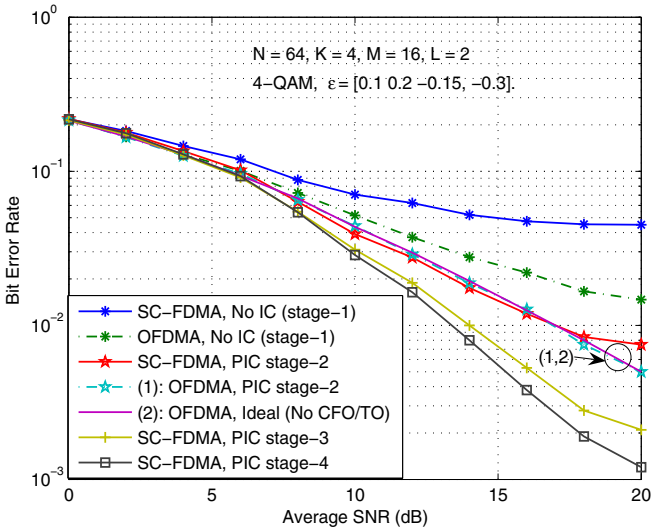

Fig. 3. Comparison of BER performance between SC-FDMA and OFDMA with CFO. $N = 64$, $K = 4$, $M = 16$, 4-QAM, $L = 2$, $\epsilon = [0.1, 0.2, -0.15, -0.3]$. No TO. User 1 is desired user. *SC-FDMA (without IC) performs worse than OFDMA in the presence of CFO. With the proposed PIC, however, SC-FDMA recovers its frequency diversity advantage and outperforms OFDMA.*

where $\widehat{\mathbf{x}}^{u,m-1}$ are the estimates of respective symbols in the previous stage.

IV. Simulation Results and Discussions

In this section, we present the simulation results on i) uncoded BER performance without and with PIC receiver in SC-FDMA with MMSE equalizer for no CFOs and TOs (i.e., perfect alignment), and ii) uncoded BER performance without and with PIC receiver in SC-FDMA and OFDMA with CFOs only and with CFOs and TOs. The parameters used in all the simulations are: $N = 64$, $K = 4$, $M = 16$, $L = 2$, 4-QAM, and interleaved allocation. Perfect knowledge of the CIRs of all the users is assumed.

In Fig. 2, we present the uncoded BER performance of the proposed PIC receiver for SC-FDMA with MMSE equalizer

978-1-4244-4148-8/09/$25.00 ©2009
This full text paper was peer reviewed at the direction of IEEE Communications Society subject matter experts for publication in the IEEE "GLOBECOM" 2009 proceedings.

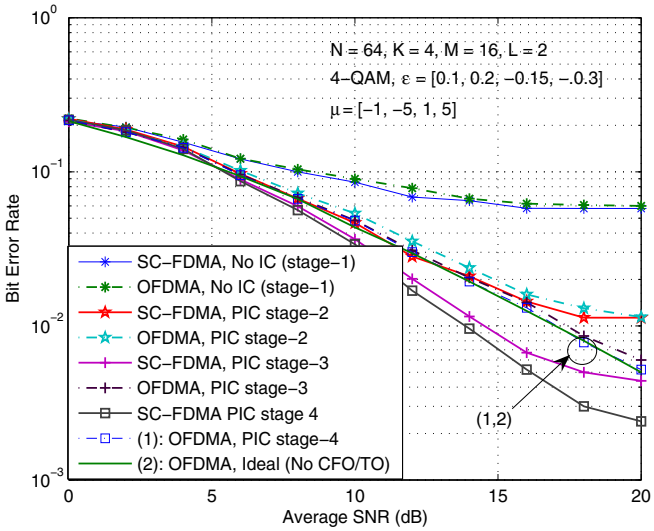

Fig. 4. Comparison of BER performance between SC-FDMA and OFDMA with CFO and TO. $N = 64$, $K = 4$, $M = 16$, 4-QAM, $L = 2$, $\epsilon = [0.1, 0.2, -0.15, -0.3]$, $\mu = [-1, -5, 1, 5]$. User 1 is desired user. *With the proposed PIC, SC-FDMA recovers its frequency diversity advantage and outperforms OFDMA.*

for the case of perfect alignment (i.e., no CFO/TO), as a function of SNR. From Fig. 2, we observe that the PIC receiver, even with one cancellation stage, is able to improve the performance of the receiver without PIC by removing the residual interference present at the MMSE equalizer output (i.e., MMSE-SI described in Sec. III-A). For example, at 20 dB SNR, the BER with no IC is 1.5×10^{-3}, which improves to 6×10^{-4} with once stage of the proposed cancellation..

Figure 3 shows the uncoded BER performance of SC-FDMA and OFDMA without and with the proposed PIC for the case with CFOs and no TO, as a function of SNR. The CFOs of different users are, $[\epsilon_1, \epsilon_2, \epsilon_3, \epsilon_4] = [0.1, 0.2, -0.15, -0.3]$. Perfect knowledge of CFOs of all the users is assumed at the receiver. The BER performance of OFDMA in the ideal case of no CFOs/TOs is also plotted. From Fig. 3, we can observe the following. Without interference cancellation (i.e., stage-1) both SC-FDMA and OFDMA exhibit high error floors due to CFO-induced MUI. The BER in OFDMA is better than that in SC-FDMA (e.g., 1.5×10^{-2} BER at 20 dB SNR in OFDMA versus 4.5×10^{-2} BER in SC-FDMA for the same SNR). With the proposed PIC, there is a significant improvement in the BER performance of both SC-FDMA and OFDMA. In OFDMA, the BER at the 2nd stage output almost reaches OFDMA's ideal performance corresponding to no CFOs and TOs. On the other hand, in SC-FDMA, the proposed PIC with increased number of stages (3rd and 4th stages) significantly outperforms even the ideal performance in OFDMA, illustrating the ability of the PIC to restore the frequency diversity effect in SC-FDMA. Figure 4 shows a similar uncoded BER comparison between SC-FDMA and OFDMA in the presence of both CFOs as well as TOs, where the TOs for different users are taken to be $[\mu_1, \mu_2, \mu_3, \mu_4] = [-1, -5, 1, 5]$ and perfect knowledge of these TOs is assumed at the receiver. Like Fig. 3, Fig. 4 also illustrates the superiority of SC-FDMA over OFDMA in terms of uncoded BER performance when three or more stages of the proposed PIC are used.

V. Conclusions

We investigated the effect of large CFOs and TOs on the uncoded BER performance of SC-FDMA systems with MMSE equalization. We illustrated the degradation in performance due to the self interference and multiuser interference terms caused due to the MMSE equalization operation in SC-FDMA. Since these MMSE equalization induced interference terms are not there in OFDMA, SC-FDMA performed poorly compared to OFDMA. However, through the use of the proposed PIC, the uncoded BER performance of SC-FDMA with MMSE equalization even with large CFOs and TOs was shown to be better than that of the ideal OFDMA performance (with no CFO/TO), due to the frequency diversity effect in SC-FDMA. This illustrates the effectiveness of the proposed PIC and the need for such cancellers in SC-FDMA to achieve better performance than OFDMA. The present work can be further extended to consider coded BER performance, effect of imperfect knowledge of CFOs/TOs and channel coefficients.

References

[1] E. Sofer and Y. Segal, "Tutorial on multi-access OFDM (OFDMA) technology." *DOC: IEEE 802.22-05-0005r0*.

[2] H. G. Myung, J. Lim, and D. J. Goodman, "Single carrier FDMA for uplink wireless transmission," *IEEE Veh. Tech. Mag*., vol. 1, no. 3, pp. 30-38, September 2006.

[3] H. Sari, G. Karam, and I. Jeanclaude, "Frequency domain equalization of mobile radio and terrestrial broadcast channels," *Proc. IEEE GLOBECOM'94*, vol. 1, November 1994.

[4] A. Czylwik, "Comparison between adaptive OFDM and single carrier modulation with frequency domain equalization," *Proc. IEEE VTC'97*, vol. 2, pp. 865-869, May 1997.

[5] M. Tanno, Y. Kishiyama, N. Miki, K. Higuchi, and M. Sawahashi, "Evolved UTRA - physical layer overview," *Proc. IEEE Signal Process. Advances in Wireless Commun.*, pp. 1-8, June 2007.

[6] 3GPP TR 25.814 V1.4.0 (2006-05), *Physical layer aspects for evolved UTRA*. http://www.3gpp.org.

[7] 3GPP TS 36.211, *Evolved Universal Terrestrial Radio Access (E-UTRA); Physical Channels and Modulation, Release 8)*, June 2007. http://www.3gpp.org.

[8] B. E. Priyanto, H. Codina, S. Rene, T.B. Sorensen, and P. Mogensen, "Initial performance evaluation of DFT-spread OFDM based SC-FDMA for UTRA LTE uplink," *Proc. IEEE VTC'2007*, pp. 3175-3179, April 2007.

[9] G. Berardinelli, B. E. Priyanto, T. B. Sorensen, and P. Mogensen, "Improving SC-FDMA performance by Turbo equalization in UTRA LTE uplink," *Proc. IEEE VTC'2008 (Spring)*, pp. 2557-2561, May 2008.

[10] W. H. Gerstacker, P. Nickel, F. Obernosterer, U. L. Dang, P. Gunreben, and W. Koch, " Trellis-based receivers for SC-FDMA transmission over MIMO ISI channels," *Proc. ICC'2008*, pp. 4526-4531, May 2008.

[11] H. Wang, X. You, B. Jiang, and X. Gao, "Performance analysis of frequency domain equalization in SC-FDMA systems," *Proc. ICC'2008*, pp. 4342-4347, May 2008.

[12] C. Ciochina, D. Mottier, and H. Sari, "An analysis of three multiple access techniques for the uplink of future cellular mobile systems," *European Trans. on Telecommun.*, pp. 19:581-588, June 2008.

[13] D. Haung and K.B. Lataief, "An interference cancellation scheme for carrier frequency offsets correction in OFDMA systems," *IEEE Trans. Commun.*, vol 53, no.7, pp. 1155-1165, July 2005.

[14] R. Fantacci, D. Marabissi, and S. Papini, "Multiuser interference cancellation receivers for OFDMA uplink communications with carrier frequency offset," *Proc. IEEE GLOBECOM'04*, pp. 2808-2812, 2004.

[15] S. Manohar, D. Sreedhar, V. Tikia, and A. Chockalingam, "Cancellation of multiuser interference due to carrier frequency offsets in uplink OFDMA," *IEEE Trans. Wireless Commun.*, July 2007.

[16] K. Raghunath and A. Chockalingam, "SIR analysis and interference cancellation in uplink OFDMA with large carrier frequency and timing offsets," *IEEE Trans. Wireless Commun.,* vol. 8, no. 5, pp. 2202-2208, May 2009.

[17] IEEE 802.16e-2005: IEEE standard for Local and Metropolitan Area Networks. Part 16: Air Interface for Fixed and Mobile Broadband Wireless Access Systems. Amendment 2: Physical and Medium Access Control Layers for Combined Fixed and Mobile Operation in Licensed Bands. December 2005.

978-1-4244-4148-8/09/$25.00 ©2009
This full text paper was peer reviewed at the direction of IEEE Communications Society subject matter experts for publication in the IEEE "GLOBECOM" 2009 proceedings.